Electronic structure and bonding properties of titanium silicides

Mathias Ekman and Vidvuds Ozoliņš
Theoretical Physics, Royal Institute of Technology, SE-100 44 Stockholm, Sweden
(Received 30 September 1997)

We present an *ab initio* full-potential linear muffin-tin orbital study of the structural and electronic properties of seven compounds of the binary Ti-Si system. The calculations were done with the compounds in their proposed stable structures, which are $A3$ Ti, $D8_8$ Ti_5Si_3, $B27$ TiSi, TiSi in distorted $L1_0$, $C49$ $TiSi_2$, $C54$ $TiSi_2$, and $A4$ Si. The calculated enthalpies of formation reproduce the observed sequence of stable structures and agree reasonably well with the values deduced from experiments. The paper ends with an analysis of the electronic structure and the bonding in the stable phases, which shows that the properties of the experimentally observed stable phases differ considerably from those of the hypothetical unstable structures. Therefore, the latter represent a poor model for the bonding in some of the stable Ti-Si compounds. We suggest that the bonding in these structures has a complex character extending beyond simple Ti-Ti and Ti-Si pairwise interactions. [S0163-1829(98)06707-1]

I. INTRODUCTION

The extensive study[1–16] of transition-metal silicides is related to their applications in silicon technology as Ohmic contacts, low-resistivity interconnects, and Schottky barriers. The refractory disilicides RSi_2 (R in groups IV-VI) are especially attractive in such applications because of their high-temperature stability and their high electrical conductance. The major interest has been in the group-VIII disilicides $CoSi_2$ and $NiSi_2$. Unlike the refractory disilicides these form in high-symmetry structures, which has made an intense study possible. Recently there has been a growing interest in iron silicides,[5,6] mainly because the semiconducting stable phase β-$FeSi_2$ can be used in optoelectronic devices. The refractory disilicide $TiSi_2$, in the $C54$ structure, is an excellent candidate for applications in intergrated circuit interconnection schemes,[17] and is today the most commonly used silicide in the 0.35-μm generation of circuits.[18] Other crystalline titanium silicides are interesting because they are corrosion-resistive compounds. The Ti-Si system has also received interest as an amorphous alloy.[19]

The theoretical studies[12–14] have been focused on $TiSi_2$. Some attempts, with the use of high-symmetry crystal structures, have been made to understand the electronic structure in TiSi and Ti_3Si.[10] Because of the crucial interplay between structure and bonding we have instead studied the proposed stable low-symmetry structures. This will give a better picture of the electronic structure and the bonding properties in this system.

The understanding of the bonding in transition-metal silicides[20] can be found in terms of covalent hybridization of atomic states and the increase of the dd bond length. When a transition-metal element and a Si atom are brought together, the metal-d states hybridize with the p states forming a bonding hybrid that is more tightly bound than either of the states from which it is formed. Not all of the d states will have the correct symmetry to form these bound hybrids, resulting in nonbonding states. The increase in the dd bond length, caused by the insertion of the Si atoms, will decrease the d band broadening contribution to the stability of the lattice.

This paper is organized as follows. Section II reviews the crystal structures of the titanium silicides. Our *ab initio* calculations and the resulting equilibrium structural parameters of the Ti-Si system are presented in Sec. III. Finally the results of our examination of the electronic structure are presented in Sec. IV.

II. THE BINARY SYSTEM Ti-Si

A. Stable phases

The Ti-Si phase diagram,[21] exhibits the following ordered phases: Ti_3Si, Ti_5Si_3, Ti_6Si_4, Ti_5Si_4, TiSi, and $TiSi_2$. This paper does not treat the three phases Ti_3Si, Ti_6Si_4, and Ti_5Si_4, due to the large number of atoms per unit cell. The investigated stable phases and their structural data are presented in Table I. In the ''site'' column we give the Wyckoff letters. The sum of multiplicities is the number of atoms per conventional unit cell. This should be divided by 1, 2, and 4 to obtain the value for the primitive cell for space groups starting with P, C, and F, respectively. The ''special position'' is given in a fraction of the basis vector (multiplied with 1000 or 10 000). A complete list of all other points in the Wyckoff set is given elsewhere.[22]

B. Geometry

Throughout this paper we use the *Strukturbericht* labels[22] $A3$, $D8_8$, $B27$, $C54$, $C49$, $A4$ for Ti, Ti_5Si_3, TiSi in FeB structure, $TiSi_2$ in $TiSi_2$ structure, $TiSi_2$ in $ZrSi_2$ structure, and Si phases, respectively. Where this is not possible, i.e., for the distorted $L1_0$ propsed by Ageev and Samsonov, we use the notation AG. Figures 1–5 give projections for the treated phases. In all figures the small circles are Si atoms and the large ones are Ti atoms. The shading of the circle indicates the height above the projection plane. From white to black this is 0, $\frac{1}{4}$, $\frac{1}{2}$, and $\frac{3}{4}$ of the lattice vector normal to the plane. Throughout this section distances are based on the experimental volume.

TABLE I. Structural data (Ref. 26) for the treated TiSi phases.

Composition	Structure	Space group	Site		Special position			R_{MT}	Prototype
Ti	$A3$	$P6_3/mmc$	Ti	$2a$	0	0	0	2.64	Mg
Ti_5Si_3	$D8_8$	$P6_3/mcm$	Ti_1	$4d$	333	667	000	2.42	Mn_5Si_3
			Ti_2	$6g$	240	000	250	2.30	
			Si	$6g$	615	000	250	2.42	
TiSi	$B27$	$Pnma$	Ti	$4c$	179	250	127	2.85	FeB
			Si	$4c$	030	250	620	2.05	
	AG	$Pmm2$	Ti_1	$1a$	0	0	0	2.265	TiSi
			Ti_2	$1b$	000	500	000	2.17	
			Ti_3	$1c$	500	000	500	2.30	
			Ti_4	$1d$	500	500	500	2.55	
			Si_1	$2g$	000	766	625	2.27	
			Si_2	$2h$	500	288	078	2.17	
$TiSi_2$	$C54$	$Fddd$	Ti	$8a$	0	0	0	2.43	$TiSi_2$
			Si	$16e$	3365	0	0	2.39	
	$C49$	$Cmcm$	Ti	$4c$	0000	1022	2500	2.65	$ZrSi_2$
			Si_1	$4c$	0000	4461	2500	2.00	
			Si_2	$4c$	0000	7523	2500	2.00	
Si	$A4$	$Fd\overline{3}m$	Si	$8a$	125	125	125	2.22	Diamond

Figure 1 shows an ab projection of the hexagonal structure $D8_8$. From Table I we see that $D8_8$ has Ti atoms in two inequivalent sites ($4d$ and $6g$). In Fig. 1 these correspond to the white and dark gray ($4d$) and the black and light gray ($6g$) circles. Ti_1 has two Ti_1 first neighbors, six Si second neighbors, and six Ti_2 third neighbors [$d^{(1)}=4.86$ ($=c/2$), $d^{(2)}=4.99$, $d^{(3)}=5.97$ a.u.]. Ti_2 has two Si first neighbors, three Si second neighbors, two Ti_2 third neighbors, four Ti_2 fourth neighbors, and four Ti_1 fifth neighbors ($d^{(1)}=4.73$, $d^{(2)}=5.27$, $d^{(3)}=5.83$, $d^{(4)}=5.91$, $d^{(5)}=5.97$ a.u.). Si has two Ti_2 first neighbors, four Ti_1 second neighbors, three Ti_2 third neighbors, and four Si fourth neighbors ($d^{(1)}=4.73$, $d^{(2)}=4.99$, $d^{(3)}=5.27$, $d^{(4)}=7.27$ a.u.).

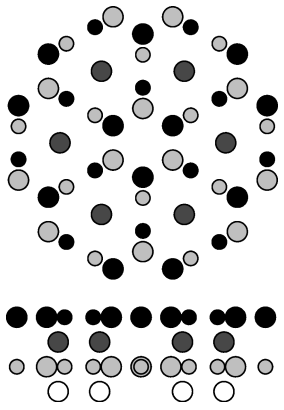

FIG. 1. ab projection and side view for $D8_8$.

Figure 2 shows the $B27$ structure. Each Ti atom has seven Si atoms in the range of 4.92–5.13 a.u. and six Ti atoms at 6.06 a.u. The Si atoms have two nearest Si atoms, with $d^{(1)}=4.18$, which is 95% of the distance in $A4$, and eight Ti atoms within the range 4.92–5.13 a.u.

Figure 3 shows the structure proposed by Ageev and Samsonov.[23] The structure resembles the $L1_0$ structure, with the positions of the Si somewhat distorted.

The refractory disilicides form a variety of complicated, low-symmetry structures. Despite their differences, they share a common structural element, nearly hexagonal RSi_2 layers.[24] $TiSi_2$ forms in two structures, the orthorhombic structures $C54$ and $C49$. A common feature of these structures is that each Ti atom is surrounded by ten Si atoms.

Figure 4 shows a projection of the conventional unit cell onto the ab plane for $C54$. This structure is face-centered tetragonal. The layer structure is just an $ABCD$ stacking of equivalent planes (the $C11_b$ is the AB stacking with the same registry). Ti has four Si first neighbors, four Si second neighbors, two Si third neighbors, and four Ti fourth neighbors

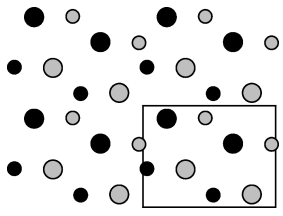

FIG. 2. cb projection for $B27$.

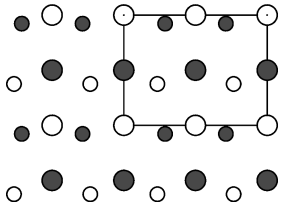

FIG. 3. cb projection for AG.

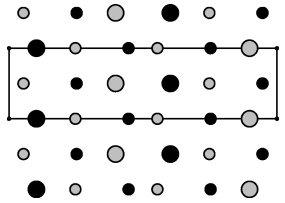

FIG. 5. ab projection for $C49$.

($d^{(1)}=4.83$, $d^{(2)}=5.21$, $d^{(3)}=5.26$, $d^{(4)}=6.06$ a.u.). Si has two Si first neighbors and two Ti second neighbors ($d^{(1)}=4.79$, $d^{(2)}=4.83$ a.u.).

Figure 5 shows the other structure at 67% Si, $C49$. This structure is just a two-layer stacking (AB'), but with different registry than that in $C54$. Each layer looks very similar to that of $C54$, being just stretched along the b axis. Each Ti atom has four Si atoms as nearest neighbors ($d^{(1)}=4.98$) and ten Si atoms in the range 4.98–5.31 a.u. The nearest Ti-Ti distance is $d^{(5)}=6.31$. Si_1 has four first Si_1 neighbors and two Ti second neighbors ($d^{(1)}=4.83$, $d^{(2)}=5.09$ a.u.). Si_2 has two first Si_2 neighbors and four Ti second neighbors ($d^{(1)}=4.41$, $d^{(2)}=4.98$ a.u.).

Note that in the case of $D8_8$ the Ti-Ti nearest-neighbor distance is just 89% of that in $A3$. Assuming that the dd interatomic matrix elements decrease as the fifth power of the distance,[25] they should be about 80% larger in $D8_8$ than in $A3$.

C. Hypothetical structures

For comparison calculations were done for some earlier used hypothetical high-symmetry structures. These structures were Ti_3Si in $L1_2$, TiSi in NaCl and $L1_0$, $TiSi_2$ in $C11_b$, and $TiSi_3$ in $L1_2$.

III. CALCULATION METHOD

Our calculations were done with a full-potential version of the linear muffin-tin orbital (LMTO) method[27,28] with nonoverlapping spheres. The contributions from the interstitial region were accounted for by expanding the products of Hankel functions in a series of atom-centered Hankels of three different kinetic energies. The corrected tetrahedron method[29] was used for Brillouin zone integration. Electronic exchange and correlation contributions to the total energy were obtained from the local-density functional[30] calculated by Ceperley and Alder[31] and parametrized by Vosko, Wilk, and Nusair.[32]

Three LMTO envelopes were used with the tail energies -0.01, -1, and -2.3 Ry. In the first two of these, s,p,d orbitals were included and in the last one only s and p were used. It was necessary to treat the Ti $3p$ and $3s$ states as semicore states, i.e., to do a so-called two-panel calculation.

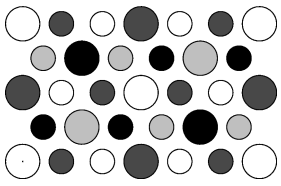

FIG. 4. ab projection for $C54$.

The basis set for the second panel consisted of $3s$, $3p$, $3d$ orbitals on the Ti sites and $3s$, $3p$ orbitals on the Si sites. The muffin-tin radii are given in Table I. These radii lead to packing fractions of 0.72, 0.54, 0.66, 0.50, 0.56, 0.61, and 0.34 for the $A3$, $D8_8$, $B27$, TiSi in TiSi, $C49$, $C54$, and $A4$, respectively. To decrease the volume of the interstitial region in the diamond structure Si, empty spheres were included in the usual way. The quality of the **k**-point mesh in the corrected tetrahedron method is determined by $\Delta k_i=|\mathbf{b}_i|/nkp_i$, where nkp_i is the number of k points along $\mathbf{b}_i$. In a single calculation the number of k points along the different basis vectors was chosen in such a way that $\Delta k_1=\Delta k_2=\Delta k_3$. The same quality k mesh was used in all calculations to ensure maximum cancellation of numerical errors and to obtain accurate energy differences. Calculations show that the error in the total energy is less than 1 mRy/atom with respect to the k-space integration error.

To be consistent, the minimum energies from the LMTO program were used even though this underestimated the lattice constant. Murnaghan's equation of state was used to determine bulk moduli and equilibrium volumes. The self-consistency loop was converged within 1 mRy/atom.

In our calculations we used experimental values[26] for all internal parameters of the proposed stable structures. To obtain the true theoretical equilibrium structure one should relax the structure with respect to all its internal parameters. In the Ti-Si system this is a horrible task when we have 2–4 coordinates and the c/a and b/a dependence of the total energy, but in the case of the hypothetical structure $C11_b$ we have relaxed the structure with respect to the c/a ratio.

A. Density of states (DOS)

In Fig. 6 we present the total DOS for the treated Ti-Si structures. In the case of $TiSi_2$ our results agree well with

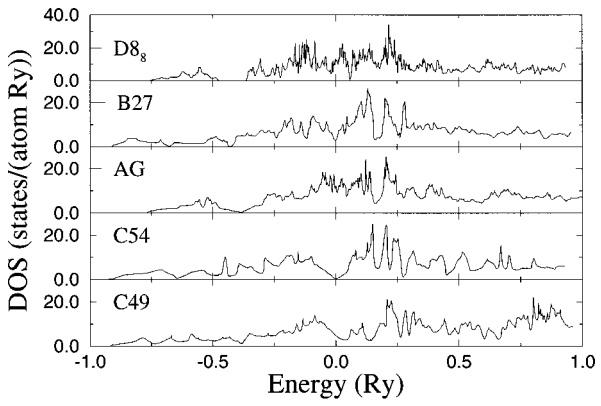

FIG. 6. Total DOS for the different phases. From the top to the bottom: $D8_8$, $B27$, AG, $C49$, and $C54$.

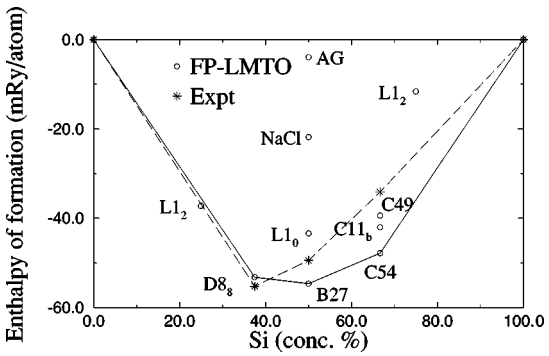

FIG. 7. The calculated and experimental values for the enthalpies of formation.

other calculations.[12,13] The Fermi level is taken as the zero of energy. The DOS at the Fermi levels are [in states/(atom Ry)] 13.2 ($D8_8$), 2.80 ($B27$), 9.33 (AG), 5.41 ($C54$), and 4.46 ($C49$). For the two hypothetical structures at 50% Si the values are 4.02 and 5.35 for TiSi in NaCl and $L1_0$, respectively. We see from Fig. 6 that for all structures except AG, the Fermi level lies in a dip of the DOS, which reduces the band-structure energy, and often correlates with the structural stability.

B. ΔH, B_0, and V_0

We present here our calculated results for the equilibrium volume V_0, bulk modulus B_0, and the enthalpy of formation ΔH, for the seven compounds in the Ti-Si system. Theoretical results refer to $T=0$, uncorrected for zero-point motion, whereas experimental values refer to room temperature. Note that the extensive quantities ΔH and V_0 are reported per atom in the present paper, i.e., divided by the total number of atoms. Figure 7 shows the experimental[33] and the calculated values for the enthalpy of formation, together with the hypotetical structures. Remarkable is the very high value for the AG structure. From the size of this value it seems unreasonable that this structure would be stable. As mentioned above AG has the highest DOS at the Fermi level (for 50% Si), while $B27$ (the most stable) has the lowest value. The theoretical equilibrium volumes are presented in Table II. The values for the volumes are underestimated by a few percent in all stable structures. In Table II we give the bulk moduli for the different stuctures.[35] It can be seen from Table II that addition of Ti to pure Si and addition of Si to pure Ti has a large (63% and 26% correspondingly) effect on the bulk modulus, indicating that both d electrons of Ti and p electrons of Si have strong effect on the bonding in this system. Using the data obtained from Murnaghan's equation of state, it is possible to calculate the entalphy as a function of the pressure. At 50% Si we obtain the following transition sequence: FeB $L10$ (35 GPa) NaCl (195 GPa), where the numbers indicate the transition pressure.

IV. THE Ti-Si BOND

The nature of the chemical bond in transition-metal silicides has been extensively studied both theoretically[1–14] and experimentally.[9–11,13–15] A fundamental distinction between the bonding of Si and of many silicides is the absence of sp^3 hybridization in the silicides. Exceptions to this are $CoSi_2$ and $NiSi_2$ where the sp^3 hybrids form directed covalent bonds with the metal-d orbitals.[7–10]

One way to distinguish between ionic and covalent character of the bonding in a compound is to examine the decomposed DOS. If the bonding is strongly covalent, the states from different sites are strongly mixed and one would except the decomposed DOS to be very similar on all sites. If the bonding is primarily ionic the decomposed DOS would be very dissimilar on sites with different atoms. To deduce the amount of hybridization in the DOS we decomposed the DOS into ''site'' contributions.

Another way to characterize the degree of covalent bonding is to calculate the charge density difference, $\Delta\rho(\mathbf{r})$, which is defined by the expression

$$\Delta\rho=\rho_{\text{crystal}}-\rho_{\text{sup}},$$

where ρ_{crystal} is the self-consistent charge density obtained at our calculated equilibrium lattice constant, and ρ_{sup} is the superposition of atomic charge density at the same lattice constant. In regions of positive contribution, charge has piled up and corresponds to ''bonding'' electrons, while regions with negative contribution correspond to ''antibonding'' states. The location of the maximum in $\Delta\rho(\mathbf{r})$ relative to the electronegative atom indicates the degree of ionic bonding, or more loosely speaking the charge transfer from the cation to the anion.

In order to emphasize bonding characteristics, ''valence'' charge density results presented here exclude the core and semicore contributions.

A. Bonding in $C54$

Figure 8 shows the decomposed DOS for $C54$. At energies well below the Fermi level the dominant contribution is

TABLE II. Calculated and experimental values for the equilibrium volumes and the bulk moduli.

Composition	Structure	V_0 [(a.u.)^3/atom]		B_0 (GPa)	
		LMTO	Expt. (Ref. 26)	LMTO	Expt. (Ref. 34)
Ti	$A3$	109.7	119.2	125.3	105.1
Ti_5Si_3	$D8_8$	98.2	103.6	157.4	
TiSi	$B27$	97.3	100.4	172.2	
	AG	104.9[35]	98.5		
$TiSi_2$	$C54$	91.5	95.4	176.4	~170
	$C49$	92.9	101.0	153.9	
Si	$A4$	133.0	134.9	94.9	98.8

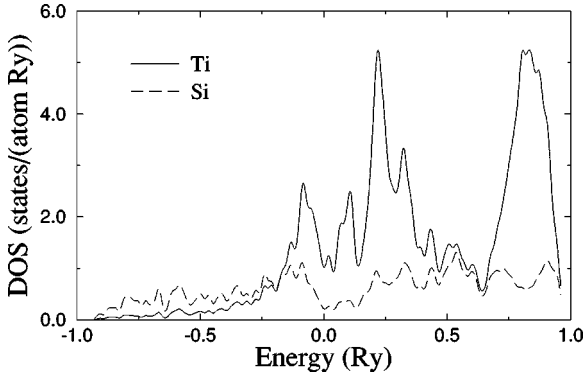

FIG. 8. Decomposed DOS for $C54$.

from the Si sites. From experiment[14] it is known that we have a concentration of Si p states in the range of 0.15–0.5 Ry below the E_F. In this region the Ti d states become important, and the two curves are covarying, suggesting the crucial role of hybridization. Next, a quasigap opens up in the Si density, which extends to ~ 0.2 Ry above E_F. Above this quasigap the Si density again starts to covary with the Ti density. The Ti states have a peak centered at the quasigap, but there is a major overlap with the two peaks of Si $3p$ character on each side of the quasigap. It has been shown[20] that the quasigap has its origin in the Ti-Si interaction. This hybridization pushes down states in energy, which results in bonding states. Some of the d states are not allowed by symmetry to form these bonding states, resulting in antibonding states above the quasigap.

B. Bonding in $D8_8$

From the decomposed DOS, presented in Fig. 9, three conclusions can be drawn. (1) The low-lying state is preferably Si $3s$. The low value from the Ti DOS in this energy range is probably due to the nonuniqueness of the site decomposition. (2) Above the gap, at -0.5 Ry, all curves follow each other, suggesting hybridization. We also see that there is a separation between the bonding and antibonding pd regions. Such separation is a characteristic of covalency.[25] (3) The two Ti curves stop following each other. If bonding only occurred between symmetry inequivalent atoms the curves should covary. This indicates bonding between equivalent atoms. To support these ideas we have calculated the charge density in different planes.

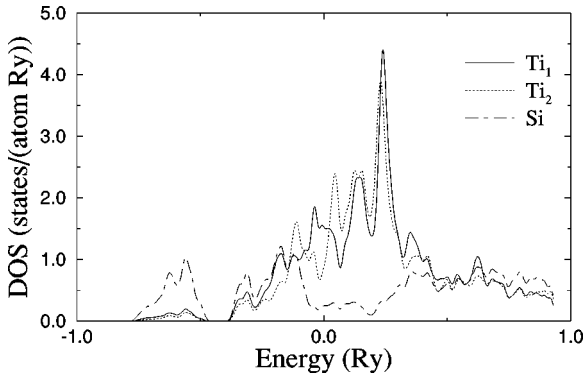

FIG. 9. Decomposed DOS for $D8_8$. Ti_1 is sited at $4d$ and Ti_2 at $6g$.

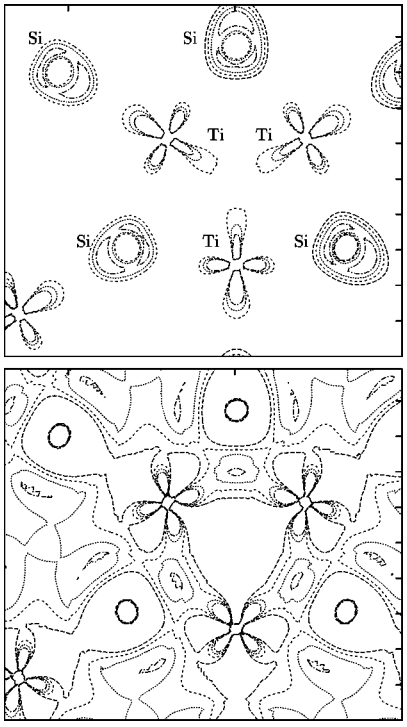

FIG. 10. Charge-density difference in the plane $z=0.75c$. The atoms are located in the center of each ''figure.'' Above: negative curves. Below: positive curves. The magitudes are 7, 5, 3, and 1 millielectrons/(a.u.)^3 for long-dashed, short-dashed, dotted, and dot-dashed lines.

Figure 10 shows $\Delta\rho$ for the [110] plane through the black atoms in Fig. 1. For clarity the negative and positive contributions have been separated into two panels. The right picture shows that charge has moved into the interstitial region in this plane. We also see that there is no direct bonding between the Ti_2 atoms. Instead one Si atom and two Ti_2 atoms bond to the region in between.

Figure 11 shows the charge density in a plane perpendicular to the ab plane. This plane goes through a Ti_1 atom and its nearest Si neighbor. To the right of the central ''column'' of Ti atoms there are two black Si atoms. Charge has moved into the interstitial region. In the lower picture, there is a region, as above, between two Ti and one Si that has gained charge. A difference is that the ''orbitals'' in the lower pic-

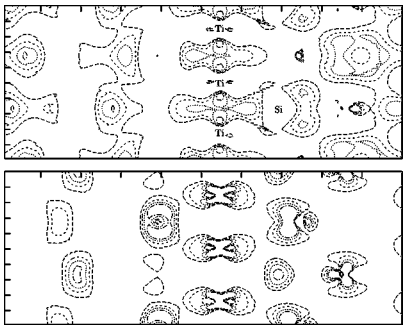

FIG. 11. Charge-density difference in the plane that contains a Ti_1 atom and its closest Si atom. The labels indicate the positions of the atoms. Above: positive curves. Below: negative curves. The magitudes are 7, 5, 3, and 1 millielectrons/(a.u.)^3 for long-dashed, short-dashed, dotted, and dot-dashed lines.

ture point towards each other, indicating direct bonding between Ti_1 atoms. As mentioned above, the dd interatomic matrix elements are about 80% lager in $D8_8$ than in $A3$.

As in the case of $C54$, there exist a quasigap in the Si density of states. The origin of the quasigap can be examined through a calculation of the DOS of the hypothetical case of Si in $D8_8$ without Ti atoms. These calculations do not show a quasigap in the DOS. From the disappearance of the quasigap with the removal of the Ti-Si coupling we argue, as in the case of $C54$, that the quasigap in the Si density is a direct result of hybridization of the Ti d states with the Si sp band.

V. SUMMARY

We have presented the result of an *ab initio* full-potential muffin-tin orbital study of the binary Ti-Si system. The enthalpies of formations and equilibrium volumes obtained from these calculations agree reasonably well with the values deduced from experiments. One of the proposed stable structures turned out to be very unstable in our calculations. Due to the low symmetry, the possibility of a more complex bonding character arises. The charge density in these phases differs considerably from that in the hypothetical unstable structures. Therefore, the latter presents a poor model for the bonding in these phases. From the analysis of the bonding in these phases it is clear that a two electron bond model can be excluded and that there is hybridization between Si sp band and the $3d$ electrons. This hybridization is responsible for the opening of a quasigap in the Si DOS.

ACKNOWLEDGMENTS

The authors want to thank G. Grimvall and J. Rundgren for valuable comments on the paper. This work was supported by the Swedish research councils NUTEK and NFR.

[1] A. K. McMahan, J. E. Klepeis, M. van Schilfgaarde, and M. Methfessel, Phys. Rev. B **50**, 10 742 (1994).
[2] L. F. Mattheiss, Phys. Rev. B **43**, 12 549 (1991).
[3] L. F. Mattheiss, Phys. Rev. B **45**, 3252 (1992).
[4] L. F. Mattheiss, Phys. Rev. B **43**, 1863 (1991).
[5] K. A. Mäder, H. von Känel, and A. Baldereschi, Phys. Rev. B **48**, 4364 (1993).
[6] L. Miglio and G. Malegori, Phys. Rev. B **52**, 1448 (1995).
[7] W. R. L. Lambrecht, N. E. Christensen, and P. Blöchl, Phys. Rev. B **36**, 2493 (1987).
[8] J. Tersoff and D. R. Hamann, Phys. Rev. B **28**, 1168 (1983).
[9] Y. J. Chabal, D. R. Hamann, J. E. Rowe, and M. Schlüter, Phys. Rev. B **25**, 7598 (1982).
[10] J. H. Weaver, A. Franciosi, and V. L. Moruzzi, Phys. Rev. B **29**, 3293 (1984).
[11] J. H. Weaver, V. L. Moruzzi, and F. A. Schmidt, Phys. Rev. B **23**, 2916 (1981).
[12] L. F. Matheiss and J. C. Hensel, Phys. Rev. B **39**, 7754 (1989).
[13] P. J. W. Weijs, M. T. Czyżyk, J. C. Fuggle, W. Seier, D. D. Sarma, and K. H. J. Buschow, Z. Phys. B **78**, 423 (1990).
[14] P. J. W. Weijs, H. van Leuken, R. A. de Groot, J. C. Fuggle, S. Reiter, G. Wiech, and K. H. J. Buschow, Phys. Rev. B **44**, 8195 (1991).
[15] P. S. Ho, G. W. Rubloff, J. E. Lewis, V. L. Moruzzi, and A. R. Williams, Phys. Rev. B **22**, 4784 (1980).
[16] H. von Känel, C. Schwarz, S. Goncalves-Conto, E. Müller, L. Miglio, F. Tavazza, and G. Malegori, Phys. Rev. Lett. **74**, 1163 (1995).
[17] S. P. Murarka, *Silicides for VSLI Application* (Academic Press, New York, 1983).
[18] M. Karen, Phys. World **11**, 35 (1995).
[19] N. Zotov and D. Parlapanski, J. Mater. Sci. **29**, 2813 (1994).
[20] C. D. Gelatt Jr., A. R. Williams, and V. L. Moruzzi, Phys. Rev. B **27**, 2005 (1983).
[21] *Binary Alloy Phase Diagrams*, edited by T. B. Massalski (American Society for Metals, Materials Park, OH, 1990), 2nd ed., Vol. 3, p. 3367.
[22] *International Tables for Crystallography*, Space-Group Symmetry, Vol. A, edited by Theo Hahn (Kluwer Academic, Dordrecht, 1989), 2nd ed.
[23] N. V. Ageev and V. P. Samsonov, Russ. J. Inorg. Chem. B **4**, 716 (1959).
[24] F. Laves, *Theory of Alloy Phases* (American Society for Metals, Metals Park, OH, 1956), p. 181.
[25] W. A. Harrison, *Electronic Structure and the Properties of Solids* (Dover, New York, 1980).
[26] W. Pearson, P. Villars, and L.D. Calvert, *Pearson's Handbook of Crystallographic Data for Intermetallic Phases* (American Society for Metals, Metals Park, OH, 1985).
[27] M. Methfessel, Phys. Rev. B **38**, 1537 (1988).
[28] M. Methfessel, C. O. Rodriguez, and O. K. Andersen, Phys. Rev. B **40**, 2009 (1989).
[29] P. E. Blöchl, O. Jepsen, and O. K. Andersen Phys. Rev. B **49**, 16 223 (1994).
[30] P. Hohenberg and W. Kohn, Phys. Rev. **136**, 864 (1964).
[31] D. M. Ceperley and B. J. Alder, Phys. Rev. B **45**, 566 (1980).
[32] S. H. Vosko, L. Wilk, and M. Nusair, Can. J. Phys. **58**, 1200 (1980).
[33] I. Barin, *Thermochemical Data of Pure Substances* (VCH, New York, 1989).
[34] C. Kittel *Introduction to Solid State Physics* 6th ed. (Wiley, New York, 1986).
[35] For TiSi in AG calculations were only done for three V/V_{exp} ratios 1.0, 1.09, and 1.12. These were then fitted to a second-order equation, from which we got the equilibrium volume ($V/V_{\text{exp}}=1.065$) and its energy. For this reason we have not calculated the bulk modulus for this structure.